Title

Quantitative modeling of STAT1 and STAT3 dynamics in IFNγ and IL-10 pathways uncovered robustness of anti-inflammatory STAT3 signaling.

Sarma U[1,2,3], Maiti M[1], Bhadange S[1], Nair A[1], Srivastava A[1], Saha B[1], Mukherjee D[1, 2].

1: National Centre for Cell Science, NCCS Complex, Ganeshkhind, SP Pune University Campus, Pune 411007, India.

2 : Corresponding author. uddipans@gmail.com , mukherjee.debasri@gmail.com

3: Present address. Labs, Persistent Systems Limited, Pingala – Aryabhata, Erandwane, Pune, 411004 India.

Abstract

Information relay by signal transduction pathways occasionally involves sharing of functionally opposing transcription factors. For instance, IFNγ-STAT1 and IL-10-STAT3 elicit pro and anti-inflammatory cellular responses, respectively, but IFNγ mediated STAT3 and IL-10 mediated STAT1 activation is also observed. Here, through experiments at the cell population level, we studied the dynamics of STAT1 and STAT3(S/1/3) in responses to both IFNγ and IL-10 stimulation and subsequently trained a simplified mathematical model that quantitatively explained the S/1/3 signal-response at different doses of IFNγ and IL-10. Next, to understand the robustness of the canonical signaling axis in each pathway, we simulated a costimulation scenario (IL-10 and IFNγ applied simultaneously) which predicted STAT3 activation would remain IL-10 driven in presence of IFNγ; subsequent experiments validated the same. We next investigated how protein expression variability may plausibly influence the robustness of IL-10-STAT3 signaling at the level of individual cells. Simulating thousands of single cells and analyzing their responses to co-stimulation we could identify emergence of two new subpopulations; in one subpopulation co-stimulation dominantly activated STAT3 and suppressed STAT1 activation, and, vice versa in the other subpopulation. Analyzing the protein concentration from these reciprocal subpopulations we found the key proteins whose cell-specific expression could control S/1/3 responses in individual cells. Taken together, we present a quantitative model that captures the signaling dynamics of STAT1 and STAT3 in response to functionally opposing cues and through single cell simulations show how reciprocal responses could emerge at the level of individual cells.

Introduction

Information encoded in the dynamics of signalling pathways triggers a plethora of biological processes like cell growth, proliferation, apoptosis or developmental lineage commitments [1-12]. A sustained (NGF stimulation) or transient (EGF stimulation) MAPK signalling dynamics, for instance, is linked to cell differentiation and proliferation [8]. Distinct dynamics of the SMAD2 transcription factors during TGFb signalling is shown to trigger either growth inhibition [13, 14] or progression of EMT[15]. In CD40 receptor signalling the MAP kinases ERK and p38MAPK are observed [11, 12] to trigger anti-inflammatory(AIF) and pro-inflammatory(PIF) cellular responses, respectively. Similarly during IL-10 signalling sustained STAT3 dynamics triggers AIF [16] whereas

transient interferon gamma(IFNγ)-STAT1 pathway elicits PIF cellualr responses[17]. However, although STAT1 and STAT3(S/1/3) are the primary responders of the IFNγ and IL-10 pathways respectively, the STATs are often observed to be cross-activated: STAT1 is activated during IL-10 [18] and STAT3 is activated during IFNγ[19] signaling. The temporal activation profiles and the regulatory mechanisms controlling the amplitude and dynamics of S/1/3 in response to both the functionally opposing cues remains less understood.

Dynamics of signal response in the IFNγ-STAT1 and IL-10-STAT3 signalling pathways are studied independently through experiments [17, 20] and mathematical modelling [21]. In IFNγ signalling transcriptionally induced negative regulators like SOCS1 and phosphatases like SHP-2 are identified as important regulators of transient STAT1 dynamics [20-24]. IL-10-STAT3 signalling lacks rapid signal termination mechanisms and negative regulation of the LI-10 signalling is observed to occur via ubiquitination, endocytosis, and degradation of the IL-10 receptor 1(IL-10R1) [25]. It however remains to be explored how different doses IFNγ and IL-10 would tune the S/1/3 signal responses and how the two pathways regulate the STATs responses in different doses. Systematic study of such dose-dependent dynamics in a signalling pathway can facilitate better understanding on the control of amplitude and duration of signalling at different activation scenarios [14, 26, 27], and further, the data can be used to calibrate mathematical models [14, 26] for gaining better insight into the plausible regulatory processes in a system. The models calibrated and validated at the cell population level can also be extended to investigate the heterogeneity of signal-response at the level of individual cells [14, 28, 29].

Here, firstly our experiments demonstrate distinct responses of S/1/3 in response to different doses of IFNγ or IL-10 stimulus. To quantitatively understand the regulatory mechanisms controlling S/1/3 dynamics we built a simplified model of IFNγ or IL-10 pathways which quantitatively captured the dynamics of S/1/3 at different doses of IFNγ and IL-10 stimuli. The calibrated model suggested signal inhibition at the receptor level, and, IFNγ dose-dependent activation of S/1/3 phosphatase [20-25], as the regulatory processes controlling the observed dynamics. Next to explore the relative robustness of the canonical signaling axis in both the pathways we simulated a co-stimulation scenario (IL-10 and IFNγ applied simultaneously). The simulations predict STAT3 amplitude would primarily remain IL-10 driven during co-stimulation which IL-10 ensures through a stronger activation of SOCS1, a negative regulator of IFNγ signaling [20-21]; subsequent experiments validated the prediction. We further extended the calibrated model to study how cell-to-cell variability in protein expression would impact the S/1/3 dynamics at the level of single cells, particularly in the co-stimulation

scenario where the canonical IL-10 could inhibits the IFNγ mediated activation of STAT3. The single cell simulations suggest, in addition to the cells exhibiting responses similar to the population level experiments, two additional subpopulations with reciprocal STAT1 and STAT3 activation profiles could emerge as a function of cell-to-cell variability. Finally, analyzing the distribution of protein concentrations from these reciprocal subpopulations we identified key proteins whose relative concentration would result in either a dominant STAT3 or STAT1 response in individual isogenic cells. We further demonstrate that with targeted minimal perturbations S/1/3 responses can be tuned further, such that, occurrence of a desired subpopulation type can either be enriched or inhibited.

Results

STAT1 and STAT3 phosphorylation in response to different doses of IL-10 and IFNγ

We took the peritoneal macrophages obtained from BALBc mice and stimulated them with increasing doses (0.5, 1.0, 2.5, 5.0, 10.0, 20.0 and 40.0 ng/ml) of either IL-10 or IFNγ ligands(details in methods). We observed: STAT1 phosphorylation is proportional to the increasing dose of IFNγ stimulation (Figure 1A) but IL-10 induced STAT1 phosphorylation showed as bell-shaped response with strongest activation at 2.5 and 5ng/ml of IL-10 (Figure 1B). STAT3 phosphorylation showed a gradual increase with escalating doses of IL-10(Figure 1B). STAT1 phosphorylation in response to IFNγ treatment is maximal and comparable between the doses 2.5-10ng/ml(Figure1A). For both IFNγ and IL-10 stimulation of 1ng/ml weak induction of the cross-activated STATs is observed; at 5ng/ml of both canonical and cross-activated S/1/3 have high phosphorylation and at 20ng/ml cross-activated STATs amplitude are inhibited in both the pathway. We selected three doses of IFNγ and IL-10: low(L), medium(M) and high(H), which are respectively 1.0 ng/ml, 5.0 ng/ml and 20.0 ng/ml, for both the ligand types to study the dose-dependent dynamic responses of the STATs. The representative immunoblots are shown in figure S1. The selected doses were also used to calibrate the S/1/3 dynamics in a simplified mathematical model comprising both IFNγ and IL-10.

Peritoneal macrophages were stimulated with L, M and H dose of IFNγ and IL-10 stimuli and S/1/3 dynamics were captured at different time points, for a total duration of 2 hours. For IFNγ treatment STAT1 phosphorylation increases as the signal strength increases, however, M and H dose don’t exhibit significant differences in phosphorylation, indicating signal saturation close to M dose upwards (Figure 1C, 1st

panel). STAT3 phosphorylation upon IFNγ stimulation exhibits a distinct profile: at M dose STAT3 is rapidly phosphorylated to a high amplitude and gets rapidly inhibited as well, but at L and H doses STAT3 phosphorylation is relatively negligible (Figure1C, 2nd panel). Such bell-shaped dynamics of signalling intermediates is also observed elsewhere [30]. In response to IL-10, the STAT1 phosphorylation peaks at M dose and a slightly inhibited response can be observed at the H dose (Figure 1D, 1st panel). Unlike STAT1 in IFNγ stimulation STAT3 amplitude decreases at the H dose of IL-10 stimulus(compare Fig. 1C, 1st panel Fig. 1D, 2nd panel). Such dose-dependent inhibition of signal-response usually indicates presence of negative regulators induced/activated as a function of applied signal [11, 14, 31, 32]. SOCS1 being a commonly induced negative regulator in IFNγ signalling [19, 20, 22 -> 21-24], we next studied SOCS1 induction upon M dose of IFNγ (Fig2E, 1st panel, dashed line). SOCS1 induction was also checked for IL-10 stimulation (Fig2E, 1st panel, solid line). Notably, SOCS1 induction upon IFNγ stimulation remains negligible, but it's stronger induction is observed upon IL-10 treatment (Fig 2E, 1st panel, solid line). The dynamics of SOCS3 induction was also captured which is a target gene downstream to both the stimulation types (Fig 2E, 2nd panel). SOCS3 in principle can also inhibit IFNγ signalling, but the relative inhibitory strength of SOCS3 is observed to be negligible compared to SOCS1 [33], hence w.r.t IFNγ stimulation we studied SOCS3 only as a target gene.

Quantitative modelling captures dynamics of STAT3 and STAT1 activation at different doses of IL-10 and IFNγ ligand

We used the observed dynamics of S/1/3 to calibrate a mathematical model comprising both IFNγ or IL-10 pathways.

The model comprises three modules

I. A Simplified receptor activation module for both IFNγ and IL-10 activation.
II. A detailed STAT1 and STAT3 phosphorylation module in response to both the IFNγ and the IL-10 stimulation.
III. A simplified transcriptional induction module where both SOCS1 and SOCS3 are induced as a function of activated STATs.

IFNγ pathway model

Figure 2A schematically shows the minimal models of IFNγ pathway. The model has a simplified step of receptor activation where details of the interaction between IFNγ Receptor(IFN-R) and the Janus kinases JAK1 and JAK2 [21] are simplified to one step

activation process [23]. As the ligand binds to the receptor the active receptor complex (IFN-LR) phosphorylates the transcription factors STAT1 and STAT3. Both the STATs undergo dimerization and forms transcriptionally active complexes [21] which in turn induces target genes such as SOCS1 and SOCS3. The time delay in transcriptional induction is captured with Hill functions [14]. Dephosphorylation of S/1/3 are assumed to be carried out by phosphatases such as SHP2[20, 36, 37] which we generically named in our model as “Phos”. We tested this simplified IFNγ model by fitting it against the dose-dependent kinetics of S/1/3. The model quantitatively captures the distinct dynamics of STAT1 phosphorylation at: L(Fig2B, 1st row, 1st column), M(Fig2B, 1st row, 2nd column) and H (Fig2B, 1st row, 3rd column) doses. Similarly, dynamics of the cross-activated STAT3 is fitted for L(Fig2B, 2nd row, 1st column), M(Fig2B, 2nd row, 2nd column) and H(Fig2B, 2nd row, 3rd column) doses. SOCS1 and SOCS3 induction kinetics at M dose was fitted together with the S/1/3 data (Fig2B, 3rd row). Details of model building and calibration is in the methods section and in the supplementary text TS1.

IL-10 pathway model

Figure 2C shows the schematics of IL-10 receptor-mediated phosphorylation of STATs and the transcriptional induction of the SOCS. Similar to the IFNγ pathway, the explicit steps of IL-10 receptor1(IL-10R1) and receptor 2(IL-10R2) binding to JAK1, Tyk2 kinases leading to the formation of active signaling complex [38] is simplified to one step activation process[25]. STAT1/3 phosphorylation steps are explicitly modeled and dephosphorylation of STAT1/3 is assumed to be carried out by a phosphatase [36,37]. Negative regulation of IL-10 receptor through degradation is considered and we named the inhibitor as IL-10Ri; such negative regulators are observed to act by sequestering the IL-10 receptor 1(IL-10R1) that subsequently leads to ubiquitination and degradation [22]. Figure 2D shows the STAT1/3 dynamics in the model upon IL-10 stimulation with L, M, and H doses. As both the pathways are built as one model with common signaling intermediates, we calibrated both IL-10 and IFNγ models simultaneously to their respective datasets. Hence, during the model calibration, the common signaling intermediates and biochemical parameters of both the pathways were constrained to have a common value that fits the S/1/3 activation in response to both stimuli.

Mechanism controlling dose dependent kinetics of the STATs

The observed bell-shaped dose response of STAT3 in both IFNγ and IL-10 stimulation, as well as the graduating pattern in activation of STAT1 for both M and H dose of IFNγ

stimulation, is captured simultoneously by our simplified model. To capture the signal-response of all the training datasets simultoneously the model required stoichiometric inhibition of IFN-LR by SOCS1 and IL-10-LR by IL-10Ri, respectively [20-25]. SOCS1 is a commonly reported feedback regulator in the IFNγ pathway but our experiments show negligible SOCS1 induction upon stimulation (Fiure1E, top panel, dotted line) and the basally present SOCS1 acts as the stoichiometric inhibitor of IFNγ signaling. Negative regulation of signal at the receptor level in both the pathways and activation of a S/1/3 phosphatase in the IFNγ pathway [20-25, 39, 40], are suggested by the model as the key regulatory processes controlling the observed S/1/3 responses.

Prediction and validation of a co-stimulation scenario: STAT3 dynamics remain robustly IL-10 driven in presence of IFNγ stimuli

As SOCS1 is strongly induced upon IL-10 but not upon IFNγ stimulation, in a scenario when both these functionally opposing pathways are simultaneously activated(co-stimulation) an IL-10 driven negative regulation of the IFNγ signaling can be expected. To quantitatively understand the consequence of IL-10 induced SOCS1 on the IFNγ pathway we next simulated both the pathways simultaneously. We chose the M doses of both the ligand types as both the canonical and cross-activated STATs are strongly activated in M dose(Figure 2B and 2D). Figure 3A depicts the co-stimulation scenario and the predictions for dynamics of STAT3(Fig 3B), STAT1(Fig 3C) and SOCS1(Fig 3C) are shown(representative immunoblots in figure S2B and S2C). To achieve robust predictions we used 40 independently fitted models with comparable goodness of fit(see in methods for details). The models predict: IL-10 induced SOCS1 would impart additional inhibition of IFNγ signaling as the excess SOCS1 would inhibit the active IFN-LR, blocking its access to S/1/3. The simulation suggest, cells subjected to both AIF (IL-10) and PIF(IFNγ) signal would robustly exhibit IL-10 driven signal response overriding the IFNγ specific activation of both the STATs. Subsequent experiments quantitatively show that STAT3 dynamics indeed remain strongly IL-10 driven as predicted by the model (Figure 3B, black filled circles). Notably, the experimentally observed STAT1 amplitude is higher than the predicted amplitude (Figure S2A) which is quantitively not in line with the initial model prediction. However, we found, despite the differences in amplitude STAT1 dynamics remain strongly comparable between the prediction and validation datasets as a quantiative match betweeen model and data was obtained by multiplying the model trajectory with a scaling factor(Figure 3C). Figure 3D shows the SOCS1 expression dynamics in co-stimulation which is closely comparable to IL-10 only stimulation scenario (compare figure 3D with figure 2D, 3rd

row, 1st column). The SOCS1 expression dynamics is also predicted using the 40 independent models with similar goodness of fit obtained using local multistate optimization [41].

Next, we asked how cell-to-cell variability in protein expression [38, 39] might influence the robustness of IL-10-STAT3 signal response. It is usually observed that isogenic cells have heterogeneity in their protein expression that subsequently results in heterogeneity in signal-response[42-45]. Such heterogeneity in signaling dynamics has phenotypic consequences; for instance, individual cells with a certain signalling state can become cancerous and in rare cases can even become drug resistant [46, 47]. Hence signal processing at the level of individual cells remain as an important topic of investigation both computationally [48] as well as experimentally [14, 44]. Based on our findings at the cell population level we next used our model to investigate if STAT3 signal-response in costimulation would remain robustly IL-10 at the level of single cells as well.

Single cell simulations show emergence of reciprocal signalling subpopulations during co-stimulation

To this end, we have extended the population-level model to understand the effect of protein expression heterogeneity(implimentation detials details in methods) on S/1/3 dynamics in co-stimulation. The single cell simulations show, in addition to cells exhibiting responses observed in the population level(called as C0 cell; in C0 cells STAT3 responses are robustly comparable between IL-10 only stimulation and co-stimulation), two distinct subpopulation of cells with functionally opposing responses emerged as consequence of cell-to-cell variability. The first subpopulation with reciprocal cell type 1(Rc-t1) has high STAT3 and low STAT1 activation(Fig 4A, 1st column, 1st and 2nd row, red line) compared to C0 cell types(Fig 4A, 1st column, 1st and 2nd row, blue line, normalized to maximum amplitude). The other subpopulation (Rc-t2) has low STAT3 and high STAT1 activation in co-stimulation(Fig 4A, 1st column, 2nd row, green line). Figure 4 shows the normalized STAT3 dynamics from C0, Rc-t1 and Rc-t2 subpopulation (for 1000 cells in each subpopulation) with their respective median and standard deviations.

To mechanistically understand how the reciprocal subpopulation emerges we analysed the protein concentration distribution in the three subpopulations to uncover the sensitivity of single-cell variables (protein concentrations) specific to a given subpopulation [14]. Figure 4B compares the distribution of the protein concentration for C0, Rc-t1 and Rc-t2 cell types. The analysis show Rc-t1 subpopulation has a high level of IL-10R and low level of IL-10Ri compared to their respective values in

C0(Figure 4B, 1st row, 1st and 2nd column), and further, the ratio of positive and negative regulator [IL-10R]/[IL-10Ri] is distinct in the cells of Rc-t1 subpopulation (Figure 4C, 1st row). Rest of the single cell variables are not strongly separable between C0 and R1-ct subpopulation (Figure 4B). On the other hand, Rc-t2 subpopulation has a relatively lower basal $SOCS1_B$ (Figure 4C, 2nd row). while rest of the variables in Rc-t2 don't exhibit sharp differences from either C0 or Rc-t1.

Mechanistically, in Rc-t1 cells stronger expression of IL-10R and a weak expression of IL-10Ri results in a stronger induction of SOCS1 through the IL-10 pathway; the abundant SOCS1, in turn, ensures stronger inhibition of IFN-LR complex. Inhibition of IFN-LR also results in lesser amount of activated S/1/3 phosphatase Phos, and consequently, a stronger and persistent STAT3 activation results. In Rc-t2 cells, weaker $SOCS1_B$ basal expression ensures lesser inhibition of IFN-LR through sequestration and a resultant increase in the level of active Phos in Rc-t2. Effect of higher level of Phos in Rc-t2 is more pronounced in STAT3 dephosphorylation (Figure 4A, compare green lines in 1st and 2nd row) which is also influenced by the respective dephosphorylation rates of STAT1 and STAT3.

Subpopulation responses can be altered by tuning only one/two critical single-cell variable

Experimental studies show protein concentration mixing [43] due to processes like cell division and the inherent noise associated to expression/degradation of proteins in individual cells [49-51] leads to stochastic changes in the cellular states of individual cells. To understand the significance of single-cell variables with distinct distribution in the three subpopulations, we next performed a set of perturbation studies where we perturbed the signalling states of cells in one subpopulation by systematically replacing the single cell variables from a subpopulation with different signalling state. As the cells in different subpopulations emerge as a function of cell-to-cell variability, this analysis is designed to systematically understand the effect of expression noise on the most sensitive proteins of the pathway. For instance, we took one C0 cell and replaced a single cell variable (like STAT1) with its counterpart from an Rc-t1 cell(C0 -> Rc-t1). To obtain good statistics a variable in one cell of C0 subpopulation is replaced with its counterpart from 1000 other cells from Rc-t1 and this was repeated for each cell of C0 subpopulation; we show 100 representative cells in the heatmaps (Figure 5). We studied the effect of such perturbations in all pairwise combinations of the subpopulations (C0 -> Rc-t1 , Rc-t2 ->C0 , C0 -> Rc-t2 , Rc-t2 -> Rc-t1 , Rc-t1 -> Rc-t2). In Figure 5A each row shows the median fraction of Rc-t1 cells transformed to a C0 cell types when a given variable in the Rc-t1 cell is replaced by its counterpart from 1000 C0 cells. The analysis show, emergence of the two reciprocal subpopulations Rc-

t1 an Rc-t2 can be attributed to the differences in the values of a small number of single-cell variables. The protein concentration distributions already show a low basal SOCS1 concentration ($SOCS1_B$) in the Rc-t2 subpopulation (Figure 4A, 2nd row, 1st column), hence, in Rc-t2 ->C0 relatively more frequent occurrences of C0 cells are observed when the SOCS1 concentration in Rc-t2 is replaced by its counterpart from C0 cells(Figure 4C, 2nd row). The analysis suggests that $SOCS1_B$ is a key determinant for the emergence of Rc-t2 subpopulation. The perturbation analysis also show significance of IFNR for the Rc-t2 -> Rc-t1 transformation (Figure 5A, 2nd row, 2nd column), which is not evident only from the protein concentration distributions (Figure4B). Next, as the ratio ILR0R/IL-10Ri is distinct in Rc-t1 we studied the effect of replacing the ratio from the other two subpopulations; figure 5B(1st row) shows the dramatic increase in the median frequency of Rc-t1 -> C0 transition when both ILR0R and IL-10Ri were simultoneously replaced from C0 to Rc-t1. Similarly, when both IFNR and its inhibitor $SOCS1_B$ is replaced between the pair of reciprocal subpopulation, the frequency of Rc-t2 -> Rc-t1 or Rc-t1 -> Rc-t2 transitions dramatically increased (compare figure 5B, 2nd row and figure 5A, 2nd row 2nd column; figure 5B, 3rd row and figure 5A, 3rd row 2nd column).

Hence our single cell analysis shows, a combinatorial change of key single-cell variables driven by the cell-to-cell variability can result in cell specific high STAT1(low STAT3) or a high STAT3(low STAT1) signalling and the robustness of IL-10-STAT3 signaling axis as observed in the cell population level would be lost, indicating a potential to generate opposing cellular responses within a population of isogenic cells.

Discussion

IL-10-STAT3 and IFNγ-STAT1 are observed to be functionally opposing a spectrum of biological processes; activation of macrophages is enhanced by STAT1 and inhibited by STAT3, cell proliferation is inhibited by STAT1 and promoted by STAT3, and in Th differentiation, STAT1 promotes Th1 responses and STAT3 inhibits Th17 response [52-58]. Transcriptionally active STAT1 induces death receptor expression to promote apoptosis and it negatively regulates the expression of several oncogenes [59, 60]; in contrast, constitutive activity of STAT3 is essential for the survival of many primary tumor cells [59]. Transcriptional targets of STAT3 are also many anti-apoptotic genes that promote tumor cell proliferation [59, 61]. Further, dynamic response of the STATs are shown to be critical in determining the cellular responses: IFNγ-STAT1 signaling or IL6-STAT3 signaling is transient and pro-inflammatory but anti-inflammatory IL-10-

STAT3 signaling is sustained [16, 23] in nature. However, despite the ability to activate functionally opposing cellular fates, experimental investigations unravel that STAT1 is also activated during IL-10 signaling and STAT3 is also activated during IFNγ signaling [18, 19, 62-64]. In this study, we firstly asked

1. How the dynamics of canonical and non-canonical STATs are regulated in the IFNγ and in the IL-10 pathway?
2. How functionally opposing cues applied simultaneously would get integrated at the level of the STATs activation?

To address these questions we conducted experiments at the cell population level, and through immunobloting, captured the kinetics of STAT1 and STAT3 activation at different doses of IFNγ and IL-10 signal. Our kinetic studies show, in addition to activating their canonical signaling partners the IFNγ and IL-10 receptors also activates the non-canonical STATs. Such cross-activated STATs, especially STAT3 activated in IFNγ exhibited very high amplitude at a M dose of IFNγ but remained significantly inhibited in both L and H doses. Thus in signal strengths around the M dose a stronger STAT3 activation through the IFNγ pathway can be expected. STAT3 activation in the canonical IL-10-STAT3 pathway also exhibits bell-shaped dose-response with maximum amplitude achieved in the M dose. The cross-activated STAT1 in response to IL-10 is weakly activated which also peaks at the M dose and in reponse to IFNγ stimuli STAT1 amplitude is highest and loweest at L and H doses respectively.

To understand the regulatory mechanisms controlling the dose-dependent activation/inhibition of the STATs we constructed a simplified mathematical model of both the IFNγ and IL-10 pathways and calibrated the model to experimental data. The model quantitatively captured the dynamics of S/1/3 in both the signaling pathways and mechanistically explains the control of S/1/3 signaling. In the IFNγ pathway negative regulation of the active signaling complex by a negative regualtor such as SOCS1 coupled to signal-dependent activation of a phosphatase explains the dose-dependent S/1/3 reponses. In IL-10 pathway negative regulation of active IL-10 receptor by a receptor inhibitor regulate the S/1/3 responses. Intriguingly, our experiments show strong SOCS1 induction upon IL-10 stimulation, but not upon IFNγ stimulation. So we next predicted a co-stimulation scenario where both IL-10 and IFNγ were applied simultaneously. The model predicted: SOCS1 induced by IL-10 would inhibit IFNγ signaling such that STAT3 amplitude and dynamics primarily remains IL-10 driven, our expriments subsequently validated the same. The robust maintenance of the primary anti-inflammatory axis (IL-10-STAT3) during co-stimulation at the cell

population level led us to investigate if similar robustness in STAT3 responses could also also be observed at the level of the single cells. Recent studies show, the signal-response at the level of single cells can determine an individual cell's fate in response to the external signal which often results in cell specific gene expression [50, 65] or phenotypic outcomes [14].

To computationally investigate the consequences of protein expression heterogeneity in S/1/3 signaling in co-stimulation we next introduced protein expression heterogenity in the population-level model [14, 28], simulated thousands of single cells, and studied the S/1/3 dynamics in individual cells. Analzing the single cell trajectories we found that in addition to cells exhibitng responses similar to population mean, where IL-10-STAT3 signaling is comarable between IL-10 only and co-stimulation, two distinct subpopulation of cells with reciprocal STAT1 and STAT3 responses emerge at the level of single cells. To understand the cellular states in the reciprocal cells we analyzed the distributions of protein concentration from differentially signaling subpopulations.

Our analysis show the two reciprocal subpopulations Rc-t1 and Rc-t2 have distinct distribution of some key variables: in Rc-t1 cells IL-10R expression is high and its inhibitor IL-10Ri is expressed in low concentration whereas in Rc-t2 cells the basal SOCS1($SOCS1_B$) is lowest among the three subpopulations. The significance of distinct distribution of IL-10R and IL-10Ri was more pronounced in Rc-t1 when we compared a ratio [IL-10R]/[IL-10Ri]. The analysis suggests that distinct subpopulation with opposing signal responses can simply emerge when one(in Rc-t2) or two(in RC-t1) key single cell variables have their concentrations in the desired range. The frequency of occurrence of each subpopulation is different but all three subpopulations can be robustly obtained in multiple independent simulations(when several thousand cells were simulated in each independent run).

Our model next explored if the reciprocal responses can be altered by altering the cellular states via targeted perturbation. It is argued that understanding the control of signal response in individual cells has the potential to help design better interventions against complex diseases like cancer[66] and to understand the mechanims of drug resistance in individual cells [67, 68]. We thus investigated if certain minimal perturbations in single cell variabiles can alter the reciprocal cellular states in a desired way. To do so we performed a perturbation analysis where we systematically swap the values of single-cell variables(one variable at a time) between the cells of a pair of subpopulation and compared the responses of a cell before and after such perturbations. We found C0 to Rc-t2 transformation or vice-versa is critically dependent on $SOCS1_B$; replacing the values of $SOCS1_B$ from cells in C0 subpopulation into cells in Rc-t2 subpopulation resulted in a significant number C0 to Rc-t2

transformation. The transformation from Rc-t1 however required simultaneous replacements of IL-10R and IL-10Ri. Our analysis sugestes, targeted inhibition/overexpression of few single-cell variables can in principle be used to enhance/inhibit STATs signal responses in a cell population. Notably, each of the three subpopulations has distinct single cell variable that critically determines the signaling state of the subpopulation; for instance, if an intervention requires more Rc-t2 cell types it can be achieved by inhibiting the basal SOCS1 expression, whereas, occurances of Rc-t1 cells can be enhanced by adjusting the ratio [IL-10R]/[IL-10Ri] through overexpression/inhibition. The single cell simulations indicate ccurrence of the reciprocal sub-population (Rc-t1 and Rc-t2) are relatively less frequent and the dominant cell types would remain as the average responders (C0), which is perhaps why we didin't observe such responses in the population median reponse (immunoblot analysis). Non-genetic cellular heterogeneity is argued as the plausible cause underlying occurrences of rare cell types with deleterious physiological consequences [46, 69, 70]. Findings from our single cell simulations may be explored further to understand the possible extremeties of responses to a given stimuli/s or drug when the target nodes are pathway elements are shared between functionally opposing signaling pathways.

Materials and methods

Experimental protocol: Balb/c derived macrophages were treated with increasing doses of recombinant IL-10 and IFNγ protein. The cells were then lysed and processed for immunoblotting. Dose response studies were used for selecting the high (20ng/ml), medium (5ng/ml) and low (1ng/ml) doses of both cytokines and kinetic studies were performed at these three selected doses.

Western blotting: After treatment with the indicated reagents, cells were washed twice with chilled PBS and lysed in cell lysis buffer [20 mM Tris (pH 7.5), 150 mM NaCl, 10%glycerol, 1mMEDTA, 1mMEGTA, 1%NonidetP-40, protease inhibitor mixture (Roche Applied Science, Mannheim, Germany) and phosphatase inhibitor mixture (Pierce)]. Lysates were centrifuged (10,500 rpm, 10mins) and supernatants were collected. Protein was quantified by using the Bradford reagent (Pierce) and an equal amount of protein was run on SDS–PAGE. Resolved proteins were blotted to PVDF (Millipore) and then blocked with 5% nonfat dried milk in TBST [25 mM Tris (pH 7.6), 137 mM NaCl, and 0.2% Tween 20]. Membranes were incubated with primary antibody at 4˚C overnight, washed with TBST, and incubated with HRP-conjugated secondary Ab.

Immunoreactive bands were visualized with the luminol reagent (Santa Cruz Biotechnology). The STAT1 antibody we used detected both splice variants of -STAT1 (Tyr701), p91 STAT1α and p84 STAT1β, here we detected STAT1α. The STAT3 antibody we used is bound to tyrosine phosphorylated STAT3 molecules of both isoforms STAT3α(86kDa) and STAT3β (79kDa).

Reagents: Antibodies specific for p-STATI (Tyr-701), STAT1, p-STAT3 (Tyr-705) and STAT3 were purchased from Cell Signaling Technology (Danvers, MA) and those for SOCS1, SOCS3 and β-actin were from Santa Cruz Biotechnology (Santa Cruz, CA). Soluble mouse recombinant IL-10 and IFNγ were procured from BD Biosciences (San Diego, CA). RPMI 1640 medium, penicillin-streptomycin and fetal calf serum were purchased from Gibco®-ThermoFisher Scientific ((Life Technologies BRL, Grand Island, NY). All other chemicals were of analytical grade.

Animals and cell culture: BALB/c mice originally obtained from Jackson Laboratories (Bar Harbor, ME) were bred in the National Centre for Cell Science's experimental animal facility. All animal usage protocols were approved by the Institutional Animal Care and Use Committee. 3% thioglycolate-elicited peritoneal macrophages were isolated from Balb/c mice and cultured in RPMI containing 10% FCS. Adherent cells were washed and maintained in a water jacketed CO2 incubator at 37^{O}C for 48hrs to allow them to reach resting stage. Serum-free medium was added to the cells for 4hrs before stimulation.

Mathematical model building:

The pathway schemes in Figure 2A and 2C and 3A were be converted to a set of ordinary differential equations (Supporting Material) which captures the dynamics of signalling in both FNγ and IL-10 pathways. We have both the pathways built within one model where we preferentially switch on either the IFNγ or IL-10 pathways for individual pathway stimulation scenarios, or activate both the pathways simultoneously in a costimulation scenario. Below we explain the model rections specific to each of pathway as well as reactions common to both the pathways.

I. Receptor activation and engagement

A. IFNγ pathway

The ligand (IFNγ) bindss to the receptor (IFNR) to form an active signaling complex IFN-LR. We lumped several steps of receptor activation[21,22] into a one step receptor activation process [23] assuming reversible kinetics .

IFNR + IFN <=> IFN-LR --------- (1)

The signling complex(IFN-LR) next carries out phosphorylation of the STAT1 and STAT3(shown in details in section 'STAT1 and STAT3 signaling', below); activates the STATs phosphatase Phos and also interact with the negative regualtor SOCS1.

STAT1 => STAT1p ; IFN-LR ---------(2)
STAT3 => STAT3p ; IFN-LR ----------(3)
Phosi => Phos ; IFN-LR ----------(4)
IFN-LR + SOCS1 <=> [IFN-LR. SOCS1] ------ (5)

While in the reactions (1) – (4), IFN-LR acts as a modifier/enzyme, reaction (5) shows sequeatraion of IFN-LR by its negative regulator SOCS1 [21] resulting in an functionally inactive complex [IFN-LR.SOCS1] that blockes the access of downstream substrats STAT1 and STAT3 to their activator IFN-LR.

B. IL10 pathway

Similar to the IFNγ pathway the IL10 receptor also binds to ligand and become functionally active. In our simplified model of the pathway the explicit receptor activation deactivation steps are simplified to a one step activation and deactivation process .

IL10R + IL10 <=> IL10-LR --------- (6)

The acive signaling complex IL10-LR phosphorylates and activates STAT3 and STAT1(explained in section 'STAT1 and STAT3 signaling', below). A receptor level inhibitor that is observed to act by targeting the IL10R1 [25] is considered in our model as the negative regualtor of IL10-LR.

STAT1 => STAT1p ; IL10-LR ---------(7)
STAT3 => STAT3p ; IL10-LR ----------(8)
IL10-LR + IL10Ri <=> [IL10-LR . IL10Ri] ------ (9)
[IL10-LR . IL10Ri] -> IL10-LR --------- (10)
[IL10-LR . IL10Ri] -> IL10Ri --------- (11)

=> IL10Ri --------- (12)
IL10Ri => ..... (13)

As observed experimetnally[25], IL10Ri production and degradation is implememted in our model as stimulation independent proesses; reaction (12) and (13) depicts the basal production and degradation of IL10Ri. The differential equations below captures the dynamics of IL10 receptor activation and its inhibition by IL10Ri.

II. STAT1 and STAT3 signaling

In addition to equations [2], [3], [7] and [8] representing the activation of IFNγ and IL-10 specific activation STAT1 and STAT3, in the third condition, co-stimulation, STAT1 and STAT3 are activated by both the stimulus types simultoneously.

STAT1 => STAT1_act ; IFN-LR , IL10-LR ----- (14)
STAT3 => STAT3_act ; IFN-LR , IL10-LR ----- (15)

Studies show competition of STAT1 and STAT3 for the active IFNγ receptor [58] which is implimented in our model. In the same lines, we implimented competition of STAT1 and STAT3 for access to IL10 (see differential equations for x8 and x10). STAT1_act and STAT3_act are the activated/phosphorylate froms of STATs which subsequently undergo dimeriazation and in turn become transcriptionally active[21]

STAT1_act + STAT1_act -> STAT1_act_Dm
STAT3_act + STAT3_act -> STAT3_act_Dm

III. Transcriptional induction of SOCS1 and SOCS3

Transcriptional induction of SOCS1 and SOCS3 were experimetnally tested upon both IFNγ and IL10 signaling. Both the SOCS are induced relatively strongly upon IL10 signaling compared to IFNγ signaling (Figure 2B and 2D), especially SOCS1 induced upon 1L10 signaling is ~3 fold higher compared to IFNγ signaling.
In our model, in absence of external signal basal production and degradation of the SOCS is given as

=> SOCS1 ----- (16)
=> SOCS3 ----- (17)
SOCS1 => ----- (18)

SOCS3 => ----- (19)

Where reaction (16)&(17) represents production and reaction (18) & (19) represents degradation of the SOCS shown.

Upon IFNγ and IL10 signaling both the SOCS are transcriptionally induced as a function of dimeric STAT1 (in IFNγ pathway) or dimeric STAT3(in IL10 pathway). Experimental studies show during IFNγ signaling in STAT1 null mice SOCS3 but not SOCS1 is induced and in STAT3 null mice SOCS3 induction is blocked [58]; thus we modeled SOCS1 and SOCS3 induction as functions STAT1_act_Dm and STAT3_act_Dm respectively. Similalry assumpotions were made for SOCS1 and SOCS3 induction in the IL10 pathway. Additionally, studies show efficient promoter binding and gene expression by STAT1 and STAT3 also depends on other complex factors like availability of other cofactors. For instance, during IFNγ stimulation, occupation of DNA-binding sites for STAT1 and the transcriptional activator Sp1 are both required for full activation of certain genes [74]. Similarly gene expression in IL10 pathway are dependent on sp1 and sp3 cofactors [75]. Also cofactors like CoaSt6 selectively enhances the expression of genes in certein pathways but not others [76] and complexity of sch regulations increase as competition of bind to different cofactors emerge between STAT1 and STAT3 [77] where expression/activation of the cofactors can be further controlled by specific input stimuli [74]. Thus it seems plausible that relative abundance of cofacators of STAT1(STAT3) for SOCS1(SOCS3) induction in IFNγ or IL10 stimualtion could be differeent. Considering the complexity of such interactions and to accomodate the plausible differences in STAT1(STAT3) mediated induction of SOCS1(SOCS3) in IFNγ and IL10 pathways we considered differerences in induction rates and Km values which were estimated during the model fitting. Differential equations below captures basal production/degradation as well as transcriptional induction dynamics of SOCS1 and SOCS3.

Model equations

The differential equations below captures the information propagation in both IFNγ and IL10 pathways. The xs' are model species and the ps are model paramters, names of the species and paramter as well as their bestfict values are detailed in supplementary table TS1.

$$\frac{d[x1]}{dt} = x5 * p2 - x1 * x2 * p1 * p44 + p46 * p47 * p44.$$

$\frac{d[x2]}{dt}$ = x5 * p2 - x1 * x2 * p1.

$\frac{d[x3]}{dt}$ = -(x5^p43* x3 * p3)/(x5^p43+ p4^p43).

$\frac{d[x4]}{dt}$ = (x5^p43 * x3 * p3)/(x5^p43 + p4^p43).

$\frac{d[x5]}{dt}$ = x1 * x2 * p1 - x5 * p2 + p44 * x6 * p6 + p44 * x6 * p17 - x5 * p44 * x11 * p5.

$\frac{d[x6]}{dt}$ = x5 * p44 * x11 * p5 - p44 * x6 * p17 - p44 * x6 * p7 - p44 * x6 * p6.

$\frac{d[x7]}{dt}$ = x4 * x8 * p9 + x4 * x13 * p9 - (x5 * p44 * x7 * p8)/(p10 * (x7/p10 + x9/p11 + 1)) - (x17 * IL10_on * x7 * p26)/(p28 * (x7/p28 + x9/p29 + 1)).

$\frac{d[x8]}{dt}$ = x4 * x13 * p9 - x4 * x8 * p9 - 2 * x8^2 * p12 + (x5 * p44 * x7 * p8)/(p10 * (x7/p10 + x9/p11 + 1)) + (x17 * IL10_on * x7 * p26)/(p28 * (x7/p28 + x9/p29 + 1)).

$\frac{d[x9]}{dt}$ = x4 * x10 * p15 + x4 * x14 * p15 - (x5 * p44 * x9 * p14)/(p11 * (x7/p10 + x9/p11 + 1)) - (x17 * IL10_on * x9 * p27)/(p29 * (x7/p28 + x9/p29 +1)).

$\frac{d[x10]}{dt}$ = x4 * x14 * p15 - x4 * x10 * p15 - 2 * x10^2 * p13 + (x5 * p44 * x9 * p14)/(p11 * (x7/p10 + x9/p11 + 1)) + (x17 * IL10_on * x9 * p27)/(p29 * (x7/p28 + x9/p29 + 1)).

$\frac{d[x11]}{dt}$ = p16 - x11 * p17 + p44 * x6 * p6 + p44 * x6 * p7 - x5 * p44 * x11 * p5 + (p44 * p20 * p16 *(x13/p30)^p41)/((x13/p30)^p41 + 1) + (IL10_on * p34 * p16 * (x14/p32)^p39)/ ((x14/p32)^p39 + 1).

$\frac{d[x12]}{dt}$ = p18 - x12 * p19 + (p44 * p21 * p18 * (x13/p31)^p42)/((x13/p31)^p42 + 1) + (IL10_on * p35 * p18 * (x14/p33)^p40)/((x14/p33)^p40 + 1).

$\frac{d[x13]}{dt}$ = x8^2 * p12 - x4 * x13 * p9.

$\frac{d[x14]}{dt}$ = x10^2 * p13 - x4 * x14 * p15.

$$\frac{d[x15]}{dt} = \text{x17 * IL10\_on * p23 + p48 * p45 * p49 - x15 * x16 * p45 * p22.}$$

$$\frac{d[x16]}{dt} = \text{x17 * p45 * p23 - x15 * x16 * p45 * p22.}$$

$$\frac{d[x17]}{dt} = \text{p45 * x18 * p25 - x17 * p45 * p23 + p45 * x18 * p37 - x17 * x19 * p45 * p24 +x15 * x16 * p45 * p22.}$$

$$\frac{d[x18]}{dt} = \text{x17 * x19 * p45 * p24 - p45 * x18 * p25 - p45 * x18 * p37 - p45 * x18 * p38.}$$

$$\frac{d[x19]}{dt} = \text{p45 * p36 + p45 * x18 * p38 - x19 * p45 * p37 + p45 * x18 * p25 - x17 * x19 * p45 * p24 .}$$

The model comprising both the pathways is calibrated to the experimental data (Figure 2), and further, the calibrated model is used for making predictions that we validated experimentally(Figure 3). Details of model calibration and validation steps can be found in supplementary file S1.

Single cell simulations

To convert the calibrated population average model to single cell level we adopted an ensemble modelling approach in which a population of single cells are generated by sampling the protein concentration assuming protein expression noise at the level of single cells follow a log-normal distribution[14, 43]. Several studies show the distribution of protein concentration in individual cells were drawn from lognormal distributions[28, 29, 43, 46], where, for a given protein its population average value from the best-fit model is used as the median of the generated single cell population.

References

1. Chen, LF, Fischle W, Verdin E, Greene WC. Duration of nuclear NF-kappa B action regulated by reversible acetylation. Science. 2001;293: 1653–1657. doi: 10.1126/science.1062374.

2. Chen YR, Wang XP, Templeton D, Davis RJ, Tan TH. The role of c-Jun N-terminal kinase (JNK) in apoptosis induced by ultraviolet C and gamma radiation – Duration of JNK activation may determine cell death and proliferation. J Biol Chem. 1996;271: 31929–31936. doi: 10.1074/jbc.271.50.31929.

3. Dolmetsch RE, Lewis RS, Goodnow CC, Healy JI. Differential activation of transcription factors induced by Ca2+ response amplitude and duration. Nature. 1997;386: 855–858. doi: 10.1038/386855a0.
4. Murphy LO, Blenis J. MAPK signal specificity: the right place at the right time. Trends Biochem Sci. 2006;31: 268–275. doi: 10.1016/j.tibs.2006.03.009.

5. Murphy LO, Smith S, Chen RH, Fingar DC, Blenis J. Molecular interpretation of ERK signal duration by immediate early gene products. Nat Cell Biol. 2002;4: 556–564. doi: 10.1038/ncb822.

6. Santos SDM, Verveer PJ, Bastiaens PIH. Growth factor-induced MAPK network topology shapes Erk response determining PC-12 cell fate. Nat Cell Biol. 2007;9: 324–330. doi: 10.1038/ncb1543.

7. Sasagawa S, Ozaki Y, Fujita K, Kuroda S. Prediction and validation of the distinct dynamics of transient and sustained ERK activation. Nat Cell Biol. 2005;7: 365–373. doi: 10.1038/ncb1233.

8. Marshall CJ. Specificity of Receptor Tyrosine Kinase Signaling – Transient Versus Sustained Extracellular Signal-Regulated Kinase Activation. Cell. 1995;80: 179–185. doi:

9. Amit I, Citri A, Shay T, Lu Y, Katz M, Zhang F, et al. A module of negative feedback regulators defines growth factor signaling. Nat Genet. 2007;39: 503-512. doi:10.1038/ng1987

10. Tullai JW, Schaffer ME, Mullenbrock S, Sholder G, Kasif S, Cooper GM. Immediate-early and delayed primary response genes are distinct in function and genomic architecture. J Biol Chem. 2007;282: 23981-23995. doi: 10.1074/jbc.M702044200.

11. Sarma U, Sareen A, Maiti M, Kamat V, Sudan R, Pahari S, et al. Modeling and experimental analyses reveals signaling plasticity in a bi-modular assembly of CD40 receptor activated kinases. PLoS One. 2012;7: e39898. doi: 10.1371/journal.pone.0039898.

12. Mathur RK, Awasthi A, Wadhone P, Ramanamurthy B, Saha B. Reciprocal CD40 signals through p38MAPK and ERK-1/2 induce counteracting immune responses. Nat Med. 2004;10: 540-544. doi:10.1038/nm1045.

13. Nicolás FJ, Hill CS. Attenuation of the TGF-beta-Smad signaling pathway in pancreatic tumor cells confers resistance to TGF-beta-induced growth arrest. Oncogene. 2003;22: 3698-3711. doi:10.1038/sj.onc.1206420

14. Strasen J, Sarma U, Jentsch M, Bohn S, Sheng C, Horbelt D, et al.Cell-specific responses to the cytokine TGFβ are determined by variability in protein levels. Mol Syst Biol. 2018;14: e7733. doi: 10.15252/msb.20177733.

15. Thiery, J.P., Acloque, H., Huang, R.Y. and Nieto, M.A. Epithelial-mesenchymal transitions in development and disease. Cell. 2009; 139: 871–890. doi:

16. Braun, Miguel Fribourg, Stuart C. Sealfon.J Biol Chem. 2013;288: 2986–2993. Cytokine Response Is Determined by Duration of Receptor and Signal Transducers and Activators of Transcription 3 (STAT3) Activation. David A.

17. Wormald S, Zhang JG, Krebs DL, Mielke LA, Silver J, Alexander WS, et al. The comparative roles of suppressor of cytokine signaling-1 and -3 in the inhibition and desensitization of cytokine signaling.
J Biol Chem. 2006;281 :11135-11143. doi:10.1074/jbc.M509595200

18. Wehinger J, Gouilleux F, Groner B, Finke J, Mertelsmann R, Weber-Nordt RM. IL-10 induces DNA binding activity of three STAT proteins (Stat1, Stat3, and Stat5) and their distinct combinatorial assembly in the promoters of selected genes. FEBS Lett. 1996;394 :365-370. doi:

19. Qing Y, Stark GR. Alternative activation of STAT1 and STAT3 in response to interferon-gamma. J Biol Chem. 2004;279 :41679-41685. doi:10.1074/jbc.M406413200.

20. Baron M, Davignon JL. Inhibition of IFN-gamma-induced STAT1 tyrosine phosphorylation by human CMV is mediated by SHP2. J Immunol. 2008;181: 5530-5536. doi:

21. Yamada S, Shiono S, Joo A, Yoshimura A.Control mechanism of JAK/STAT signal transduction pathway. FEBS Lett. 2003;534: 190-196. doi:

22 Gambin A, Charzyńska A, Miklaszewska AE, Rybiński M. Computational models of the JAK1/2-STAT1 signaling. JAKSTAT. 2013;2: e24672. doi:10.4161/jkst.24672.

23. Rateitschak K, Karger A, Fitzner B, Lange F, Wolkenhauer O, Jaster R. Mathematical modelling of interferon-gamma signalling in pancreatic stellate cells reflects and predicts the dynamics of STAT1 pathway activity. Cell Signal. 2010;22: 97-105. doi: 10.1016/j.cellsig.2009.09.019.

24. Zi Z, Cho KH, Sung MH, Xia X, Zheng J, Sun Z. In silico identification of the key components and steps in IFN-gamma induced JAK-STAT signaling pathway. FEBS Lett. 2005;579 :1101-1108. doi:10.1016/j.febslet.2005.01.009.

25. Jiang H, Lu Y, Yuan L, Liu J. Regulation of interleukin-10 receptor ubiquitination and stability by beta-TrCP-containing ubiquitin E3 ligase. PLoS One. 2011;6 :e27464. doi: 10.1371/journal.pone.0027464.

26. Vizán P, Miller DS, Gori I, Das D, Schmierer B, Hill CS. Controlling long-term signaling: receptor dynamics determine attenuation and refractory behavior of the TGF-β pathway. Sci Signal. 2013;6 :ra106. doi: 10.1126/scisignal.2004416.

27. Ahmed S, Grant KG, Edwards LE, Rahman A, Cirit M, Goshe MB, et al. Data-driven modeling reconciles kinetics of ERK phosphorylation, localization, and activity states. Mol Syst Biol. 2014;10: 718. doi: 10.1002/msb.134708.

28. Spencer SL, Gaudet S, Albeck JG, Burke JM, Sorger PK. Non-genetic origins of cell-to-cell variability in TRAIL-induced apoptosis. Nature. 2009;459: 428–432. doi:10.1038/nature08012.

29. Kallenberger SM, Beaudouin J, Claus J, Fischer C, Sorger PK, Legewie S, et al. Intra- and interdimeric caspase-8 self-cleavage controls strength and timing of CD95-induced apoptosis. Sci Signal. 2014;7 :ra23. doi: 10.1126/scisignal.2004738.

30. M Sarwar, Samuel CS, Bathgate RA, Stewart DR, Summers RJ. Serelaxin-mediated signal transduction in human vascular cells: bell-shaped concentration–response

curves reflect differential coupling to G proteins. Br J Pharmacol. 2015;172 : 1005–1019. doi:

31. Westermarck J, Li SP, Kallunki T, Han J, Kähäri VM. p38 mitogen-activated protein kinase-dependent activation of protein phosphatases 1 and 2A inhibits MEK1 and MEK2 activity and collagenase 1 (MMP-1) gene expression. Mol Cell Biol. 2001;21 : 2373-83. doi:10.1128/MCB.21.7.2373-2383.2001.

32. Srivastava N, Sudan R, Saha B. CD40-modulated dual-specificity phosphatases MAPK phosphatase (MKP)-1 and MKP-3 reciprocally regulate Leishmania major infection. J Immunol. 2011;186 :5863-5872. doi: 10.4049/jimmunol.1003957.

33. Song MM, Shuai K. The suppressor of cytokine signaling (SOCS) 1 and SOCS3 but not SOCS2 proteins inhibit interferon-mediated antiviral and antiproliferative activities. J Biol Chem. 1998;273 :35056-35062. doi:

34. Nakakuki T, Birtwistle MR, Saeki Y, Yumoto N, Ide K, Nagashima T, et al. Ligand-specific c-Fos expression emerges from the spatiotemporal control of ErbB network dynamics. Cell. 2010;141 :884-896. doi:10.1016/j.cell.2010.03.054.

35. Dalle Pezze P, Nelson G, Otten EG, Korolchuk VI, Kirkwood TB, von Zglinicki T, et al. Dynamic modelling of pathways to cellular senescence reveals strategies for targeted interventions. PLoS Comput Biol. 2014;10 :e1003728. doi:10.1371/journal.pcbi.1003728.

36. Xu D, Qu CK. Protein tyrosine phosphatases in the JAK/STAT pathway. Front Biosci. 2008;13: 4925-4932. doi:

37. Zhang J, Zhang F, Niu R. Functions of Shp2 in cancer. J Cell Mol Med. 2015;19 : 2075-2083. doi: 10.1111/jcmm.12618.

38. Riley JK, Takeda K, Akira S, Schreiber RD. Interleukin-10 receptor signaling through the JAK-STAT pathway. Requirement for two distinct receptor-derived signals for anti-inflammatory action. J Biol Chem. 1999;274 :16513-16521. doi:

39. Schaper F, Gendo C, Eck M, Schmitz J, Grimm C, Anhuf D, et al. Activation of the protein tyrosine phosphatase SHP2 via the interleukin-6 signal transducing receptor protein gp130 requires tyrosine kinase Jak1 and limits acute-phase protein expression.Biochem J. 1998;335 :557-65. doi:

40. Bachmann J, Raue A, Schilling M, Böhm ME, Kreutz C, Kaschek D, et al. Division of labor by dual feedback regulators controls JAK2/STAT5 signaling over broad ligand range. Mol Syst Biol. 2011;7 :516. doi: 10.1038/msb.2011.50.

41. Raue A, Schilling M, Bachmann J, Matteson A, Schelker M, Kaschek D, et al. Lessons learned from quantitative dynamical modeling in systems biology. PLoS One. 2013;8 :e74335. doi:10.1371/journal.pone.0074335.

42. Spencer SL, Sorger PK. Cell. Measuring and modeling apoptosis in single cells. 2011;144 :926-939. doi: 10.1016/j.cell.2011.03.002.

43. Sigal A, Milo R, Cohen A, Geva-Zatorsky N, Klein Y, Liron Y, et al. Variability and memory of protein levels in human cells. Nature. 2006;444 :643-646. doi:10.1038/nature05316.

44. Roux J, Hafner M, Bandara S, Sims JJ, Hudson H, Chai D, et al. Fractional killing arises from cell-to-cell variability in overcoming a caspase activity threshold. Mol Syst Biol. 2015;11 :803. doi: 10.15252/msb.20145584.

45. Kellogg RA, Tay S. Noise facilitates transcriptional control under dynamic inputs. Cell. 2015;160 :381-392. doi: 10.1016/j.cell.2015.01.013.

46. Shaffer SM, Dunagin MC, Torborg SR, Torre EA, Emert B, Krepler C, et al. Rare cell variability and drug-induced reprogramming as a mode of cancer drug resistance. Nature. 2017;546 :431-435. doi: 10.1038/nature22794.

47. Gupta PB, Fillmore CM, Jiang G, Shapira SD, Tao K, Kuperwasser C, et al. Stochastic state transitions give rise to phenotypic equilibrium in populations of cancer cells. Cell.2011;146: 633–644. doi:10.1016/j.cell.2011.07.026.

48. Jeschke M, Baumgärtner S, Legewie S. Determinants of cell-to-cell variability in protein kinase signaling. PLoS Comput Biol. 2013;9 :e1003357. doi: 10.1371/journal.pcbi.1003357. doi:10.1371/journal.pcbi.1003357.

49. Elowitz MB, Levine AJ, Siggia ED, Swain PS. Stochastic gene expression in a single cell. Science. 2002;297 :1183-1186. doi:10.1126/science.1070919.

50. Swain PS, Elowitz MB, Siggia ED. Intrinsic and extrinsic contributions to stochasticity in gene expression.Proc Natl Acad Sci U S A. 2002;99 :12795-12800. doi:10.1073/pnas.162041399.

51. Hilfinger A, Paulsson J. Separating intrinsic from extrinsic fluctuations in dynamic biological systems. Proc Natl Acad Sci U S A. 2011;108 :12167-12172. doi: 10.1073/pnas.1018832108. doi:10.1073/pnas.1018832108.

52. Herrero C, Hu X, Li WP, Samuels S, Sharif MN, Kotenko S, et al. Reprogramming of IL-10 activity and signaling by IFN-gamma. J Immunol. 2003;171 :5034-5041.

53. Hutchins AP, Diez D, Miranda-Saavedra D. The IL-10/STAT3-mediated anti-inflammatory response: recent developments and future challenges. Brief Funct Genomics. 2013;12 :489-498. doi: 10.1093/bfgp/elt028.

54. Murray PJ. The primary mechanism of the IL-10-regulated antiinflammatory response is to selectively inhibit transcription.Proc Natl Acad Sci U S A. 2005;102 : 8686-8691. doi:10.1073/pnas.0500419102.

55. Hu X, Ivashkiv LB. Cross-regulation of signaling pathways by interferon-gamma: implications for immune responses and autoimmune diseases. Immunity. 2009;31 : 539-550. doi: 10.1016/j.immuni.2009.09.002.

56. Rauch I, Müller M, Decker T. The regulation of inflammation by interferons and their STATs. JAKSTAT. 2013 Jan 1;2(1):e23820. doi: 10.4161/jkst.23820.

57. O'Shea JJ, Murray PJ. Cytokine signaling modules in inflammatory responses. Immunity. 2008; 28 :477-487.

58. Purvis HA, Anderson AE, Young DA, Isaacs JD, Hilkens CM. A negative feedback loop mediated by STAT3 limits human Th17 responses. J Immunol. 2014;193 :1142-1150.

59. Pensa S, Regis G, Boselli D, Novelli F, Poli V. STAT1 and STAT3 in tumorigenesis: two sides of the same coin. In: Stephanou A, ed. JAK-STAT Pathway in Disease. Austin: Landes Bioscience, 2008: 100-121.

60. Kominsky SL, Hobeika AC, Lake FA, Torres BA, Johnson HM. Down-regulation of neu/HER-2 by interferon-gamma in prostate cancer cells. Cancer Res. 2000; 60 :3904-3908.

61. Yu H, Kortylewski M, Pardoll D Crosstalk between cancer and immune cells: role of STAT3 in the tumour microenvironment. Nat Rev Immunol. 2007;7 :41-51.

62. Finbloom DS, Winestock KD. IL-10 induces the tyrosine phosphorylation of tyk2 and Jak1 and the differential assembly of STAT1 alpha and STAT3 complexes in human T cells and monocytes. J Immunol. 1995;155 :1079-1090.

63. Yamaoka K, Otsuka T, Niiro H, Nakashima H, Tanaka Y, Nagano S, et al. Selective DNA-binding activity of interleukin-10-stimulated STAT molecules in human monocytes. J Interferon Cytokine Res. 1999;19 :679-685.

64. Kaur N, Kim IJ, Higgins D, Halvorsen SW. Induction of an interferon-gamma Stat3 response in nerve cells by pre-treatment with gp130 cytokines. J Neurochem. 2003;87 :437-447.

65. Lane K, Van Valen D, DeFelice MM, Macklin DN, Kudo T, Jaimovich A, et al. Measuring Signaling and RNA-Seq in the Same Cell Links Gene Expression to Dynamic Patterns of NF-κB Activation.Cell Syst. 2017;4 :458-469.e5. doi: 10.1016/j.cels.2017.03.010.

66. Xia X, Owen MS, Lee RE, Gaudet S. Cell-to-cell variability in cell death: can systems biology help us make sense of it all?. Cell Death Dis. 2014;5 :e1261. doi: 10.1038/cddis.2014.199.

67. Saunders NA, Simpson F, Thompson EW, Hill MM, Endo-Munoz L, Leggatt G, et al. Role of intratumoural heterogeneity in cancer drug resistance: molecular and clinical perspectives. EMBO Mol Med. 2012;4 :675-684. doi: 10.1002/emmm.201101131.

68. Magee JA, Piskounova E, Morrison SJ Cancer stem cells: impact, heterogeneity, and uncertainty. Cancer Cell. 2012;21 :283-296. doi: 10.1016/j.ccr.2012.03.003.

69. Sharma SV, Lee DY, Li B, Quinlan MP, Takahashi F, Maheswaran S, et al. A chromatin-mediated reversible drug-tolerant state in cancer cell subpopulations. Cell. 2010;141 :69-80. doi: 10.1016/j.cell.2010.02.027.

70. Gupta PB, Fillmore CM, Jiang G, Shapira SD, Tao K, Kuperwasser C, et al. Stochastic state transitions give rise to phenotypic equilibrium in populations of cancer cells. Cell. 2011;146 :633-644. doi: 10.1016/j.cell.2011.07.026.

Figure legends :

Figure 1: Dose-response and kinetic studies of STAT1 and STAT3 phosphorylation upon IL-10 or IFNγ stimulation. 48 hrs rested Balb/c derived peritoneal macrophages, cultured in RPMI 1640 with 10% fetal bovine serum were subjected to serum starvation for 3hrs. The cells were stimulated with increasing concentrations (0.5ng/ml, 1.0ng/ml, 2.5ng/ml, 5.0ng/ml, 10.0ng/ml, 20.0ng/ml, 40.0ng/ml) of (A) recombinant IL-10 protein or (B) recombinant IFNγ protein for 15mins, then washed with ice-cold phosphate-buffered saline and lysed with RIPA lysis buffer containing protease and phosphatase inhibitors. The cell lysates were further processed for immunoblotting and probed for and total STAT1 and STAT3 proteins. (C) Kinetics of STAT1 and STAT3 phosphorylation by high (20ng/ml), medium (5ng/ml) and low (1ng/ml) doses of IFNγ stimulation.(D) Kinetics of STAT1 and STAT3 phosphorylation by high (20ng/ml), medium (5ng/ml) and low (1ng/ml) doses of IL-10 stimulation. (E) Kinetics of SOCS1 and SOCS3 expression on stimulation with medium dose of IL-10 or IFNγ. Data in (C-E) represents mean ± s.d. of three sets.

Figure 2: Quantitative modeling of STAT1 and STAT3 dynamics at different doses of IL-10 and IFNγ. (A) Schematic representation of the IFNγ pathway. The blunt heads solid lines represent catalysis; arrowheads with solid lines represent binding, unbinding, phosphorylation and dephosphorylation; blunt-headed dashed lines represent transcriptional induction. Upon ligand(IFN) binding the receptor(IFNR) forms an active signaling complex(IFN-LR) which triggers the activation of STAT1(STAT1→ STATp) and STAT3(STAT3 → STAT3p) through phosphorylation. STAT1p and STAT3p undergo dimerization to become STAT1p_Dm and STAT3p_Dm, respectively. Transcription induction of target genes such as SOCS1 and SOCS3 is shown. SOCS1 is a negative feedback regulator of IFNγ signaling which forms a functionally inactive complex [SOCS1.IFN-LR] and inhibits the signaling. A STAT1/3 phosphatase is also activated (Phosi → Phos) by IFN-LR. (B) IFNγ pathway in the model was calibrated to STAT1/3 activation dynamics at three different doses of applied signal 1ng/ml(L), 5ng/ml(M) and 20ng/ml(H). The pathway was also calibrated to the dynamics of SOCS1 and SOCS3 induction at M. (C) schematics of IL-10 signaling pathways in the model is shown. Notation of the arrows is kept same as described in the IFNγ pathway. Both STATs are activated by IL-10 stimulation. Upon ligand (IL-10) binding the receptor (IL-10R) forms an active complex (IL-10-LR) which activates both STATs. At the transcriptional level induction of SOCS1 and SOCS3 takes place. IL-10Ri represents an inhibitor of IL-10 signaling which acts by sequestrating and degrading

the IL-10 receptor. (D) IL-10 pathway in the model is calibrated to STAT1/3 phosphorylation dynamics at L, M and H doses of IL-10 stimuli and SOCS1, SOCS3 expression dynamics at M dose .

Figure 3. Prediction of STAT1 and STAT3 dynamics in co-stimulation (IL-10 + IFNγ).

(A) Schematic representation of the co-stimulation scenario. Here both IL-10 and IFNγ signal were applied simultaneously. The cyan and orange colored dashed lines with blunt heads represent IFNγ and IL-10 pathway specific STAT1/3 activation, respectively. The stimulus type independent process like STAT1/3 dimerization or their dephosphorylation step is shown with black colored arrows. (B) STAT3 dynamics upon co-stimulation. The shaded area shows predictions from 50 independent fits with the similar goodness of fit and the black dots represent experimental data. (C) STAT1 dynamics upon co-stimulation, shaded area shows predictions (with amplitude correction) from the 40 independent fits and black dots shows the data (D) SOCS1 induction upon co-stimulation. The shaded areas show prediction range and the black dots show experimental data.

Figure 4: Cell-to-cell variability in protein expression results in reciprocally signaling subpopulations (A) Normalized dynamics of STAT3 and STAT1 is shown from three distinct subpopulations C0, Rc-t1 and Rc-t2. STAT3 activation in a cell in C0 is closely comparable between it's IL-10-only and co-stimulation responses. Blue line shows median of the ratio $STAT3_{co\text{-}stimulation}/STAT3_{IL\text{-}10}$ (upper panel) and $STAT3_{co\text{-}stimulation}/STAT3_{IL\text{-}10}$ (lower panel) from 1000 C0 cells. Red line shows these ratios from Rc-t1 cells and green line shows the ratios from Rc-t2 cells, with 1000 cells in each subpopulation. (B) Distribution of single-cell variables(protein concentrations) in C0, Rc-t1, and Rc-t2 subpopulation with 1000 cells in each subpopulation.(C) Distribution of the most distinct variables in the Rc-t1 or Rc-t2 subpopulation is shown comparably.

Figure 5: Systematic replacement of single-cell variables identifies most sensitive perturbation targets specific to different subpopulations.

(A) Protein concentrations subjected to cell-to-cell variability were systematically replaced between the 6 pairs of subpopulations. In each heat map the x-axis direction shows the 100 representative cells from a subpopulation subjected to such parameter replacement. The notation Rc-t1 → CO, for instance, would mean single-cell variables in Rc-t1 cells are replaced with their counterparts from C0 cells, following which, we calculate the fraction of CO cell emerging from the Rc-t1 subpopulation. Each column in a row, for example in the 1st row 1st column of the heat map titled "Rc-t1 → CO", shows the number of C0 cells emerging per Rc-t1 cell when IL-10Ri is replaced from

500 other C0 cells; the result is normalized to show the fractions where fraction = 1 means replacement of IL-10Ri from 500 C0 cells to Rc-t1 would result in 500 C0 cells. For all the heat maps the same procedure is followed, the title of the heat map shows the pair of subpopulation studied and the y-direction shows the protein concentrations that were replaced between the pairs. For each protein concentration, 100 representative cells are sorted according to their observed frequency of transformation to the respective new type of cells. (B) The significance of change in activator to inhibitor ratio in either IL-10 or IFNγ pathway. Replacing both IL-10R and IL-10Ri from C0 to Rc-t1 resulted in dramatic increase in the Rc-t1 to C0 transformations, as compared to, only IL-10R or IL-10Ri replacement(compare figure 5A, heat map titled Rc-t1 → CO).

Supplementary figure.

Figure S1. Kinetic studies of STAT1 and STAT3 phosphorylation at low(L), medium(M) and high(H) dose of IL10 and IFNγ stimulation. Kinetics study of STAT1(A) and STAT3(B) phosphorylation at high (20ng/ml), medium (5ng/ml) and low (1ng/ml) doses of recombinant IL10 and IFNγ proteins. Balb/c derived macrophages were stimulated for 3', 7', 15', 30', 60' and 120' with the mentioned doses of IL10 or IFNγ, lysed and processed for immunoblot analysis of STAT1 and STAT3 phosphorylation.(C) Kinetics of SOCS1 AND SOCS3 expression on stimulation with MD of IL10 or IFNγ for 15', 30', 60' and 120' is shown.

Figure S2. STAT1 and STAT3 dynamics and SOCS transcriptional induction in co-stimulation (IL-10 + IFNγ)treatment. (A) Prediction from 40 independently fitted models with similar goodness of fit. The shaded area shows range of predictions and the blue filled circles show data. The model and data trajectories are closely comparable by multiplying the model trajectory with a scaling factor which is shown in Figure 3C. (B) Representative immunoblots for co-stimulation is shown. The experimental procedure is same as described in figure S1A or S1B. (C) Kinetics of SOCS1 and SOCS3 expression on stimulation with M dose of IL-10 or IFNγ.

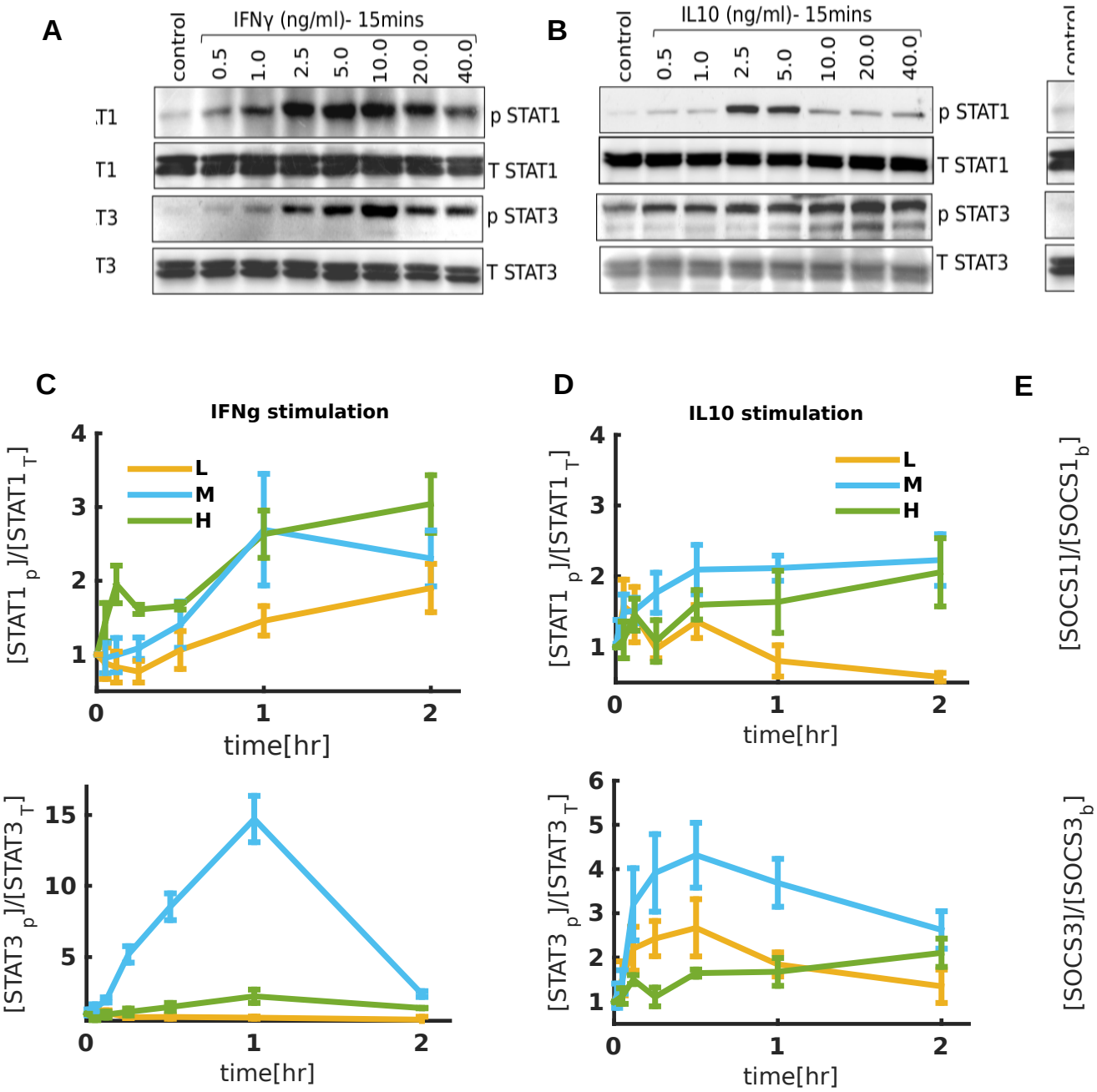
A
IFNγ (ng/ml)- 15mins
control
0.5
1.0
2.5
5.0
10.0
20.0
40.0
p STAT1
T STAT1
p STAT3
T STAT3
B
IL10 (ng/ml)- 15mins
C
IFNg stimulation
D
IL10 stimulation
E
L
M
H
IL10(M)
IFNg(M)
time[hr]

Figure 1

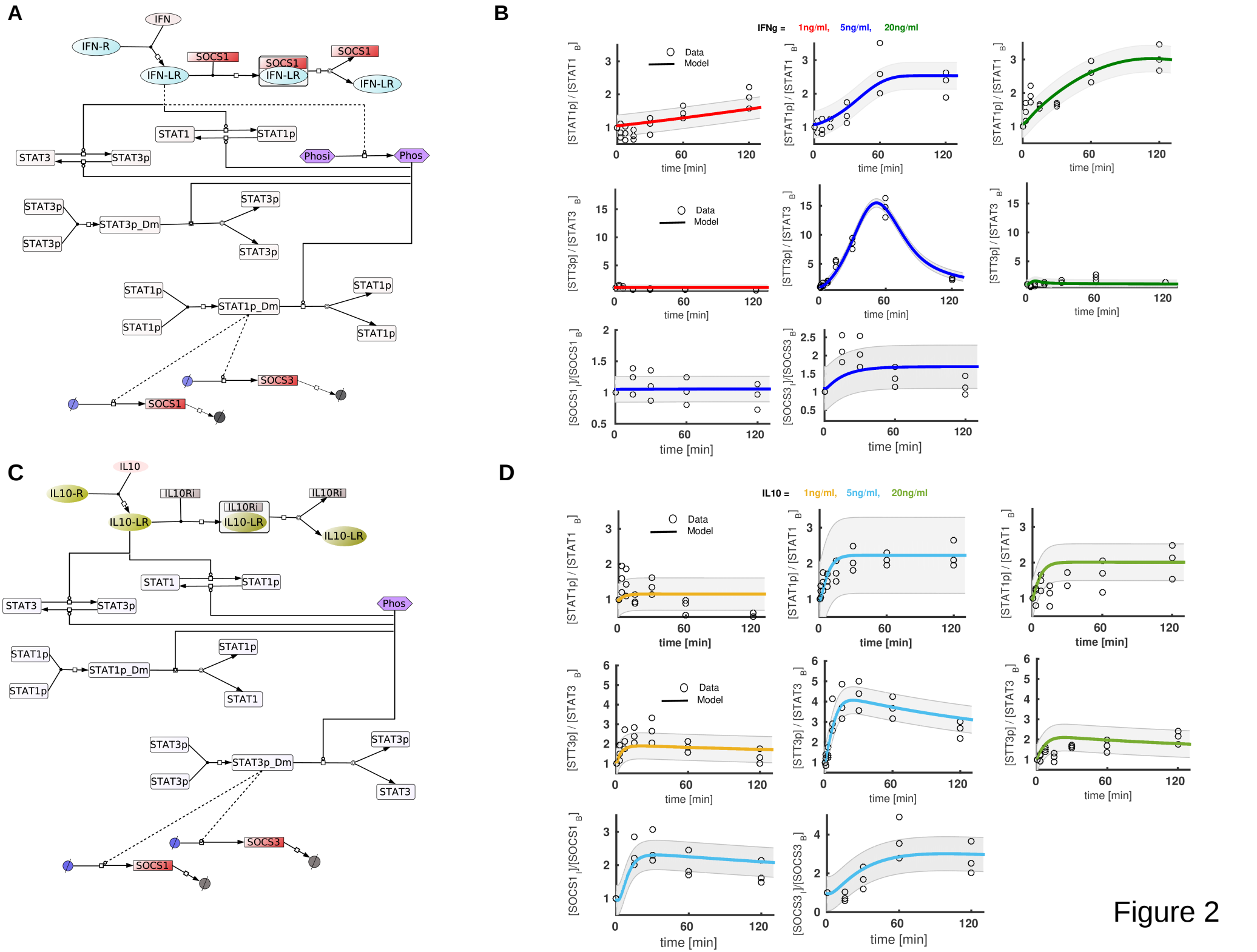
A
IFN
IFN-R
IFN-LR
SOCS1
SOCS1
IFN-LR
SOCS1
IFN-LR
STAT1
STAT1p
STAT3
STAT3p
Phosi
Phos
STAT3p
STAT3p_Dm
STAT3p
STAT3p
STAT1p
STAT1p_Dm
STAT1p
STAT1p
STAT1p
SOCS3
SOCS1
B
IFNg = 1ng/ml, 5ng/ml, 20ng/ml
Data
Model
[STAT1p] / [STAT1]B
[STT3p] / [STAT3]B
[SOCS1]/[SOCS1]B
[SOCS3]/[SOCS3]B
time [min]
C
IL10
IL10-R
IL10-LR
IL10Ri
IL10Ri
IL10-LR
IL10Ri
IL10-LR
STAT1
STAT1p
STAT3
STAT3p
Phos
STAT1p
STAT1p_Dm
STAT1p
STAT1p
STAT1
STAT3p
STAT3p_Dm
STAT3p
STAT3p
STAT3
SOCS3
SOCS1
D
IL10 = 1ng/ml, 5ng/ml, 20ng/ml
Data
Model
[STAT1p] / [STAT1]B
[STT3p] / [STAT3]B
[SOCS1]/[SOCS1]B
[SOCS3]/[SOCS3]B
time [min]

Figure 2

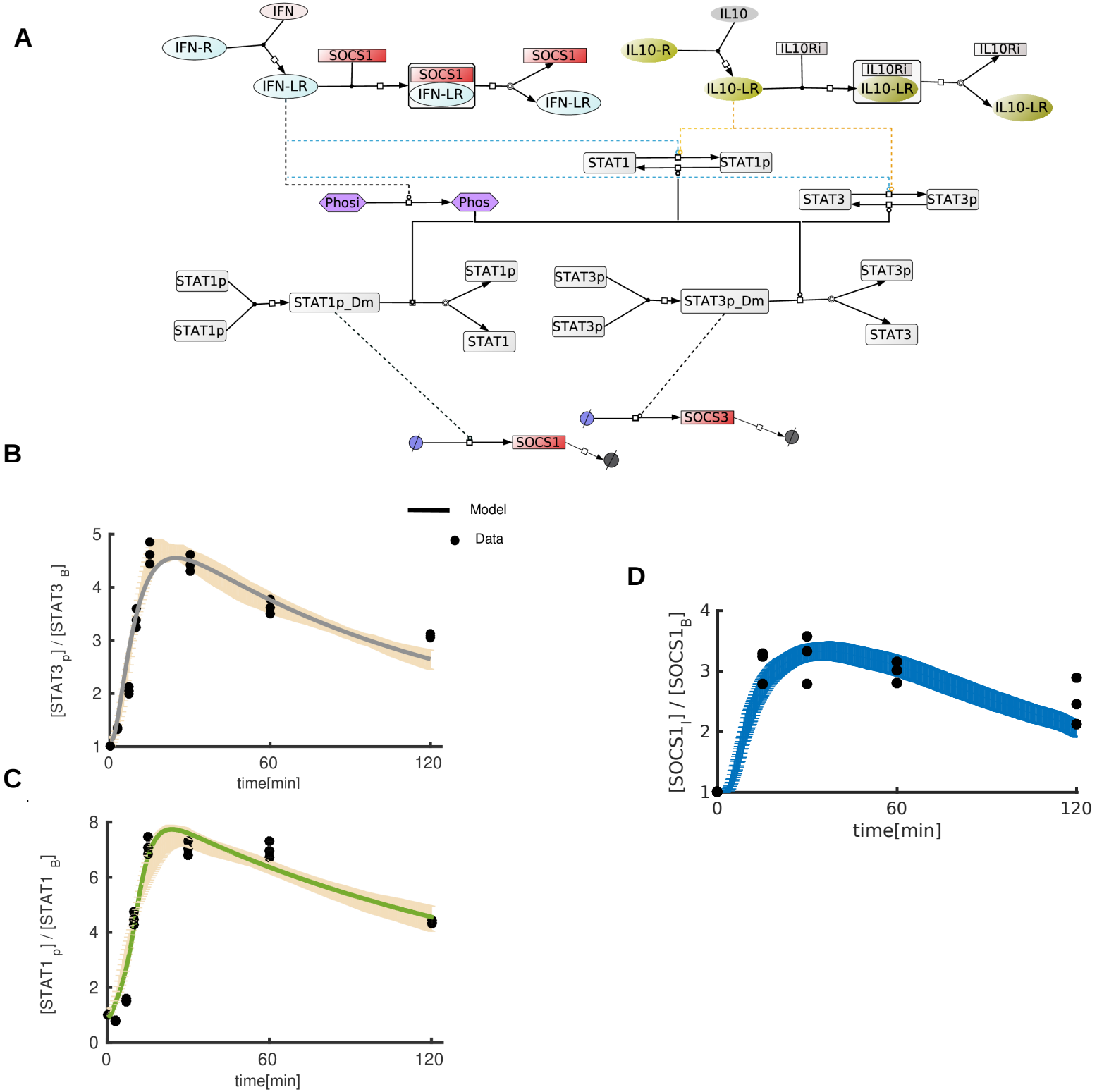
A
IFN
IFN-R
IFN-LR
SOCS1
SOCS1
IFN-LR
SOCS1
IFN-LR
IL10
IL10-R
IL10-LR
IL10Ri
IL10Ri
IL10-LR
IL10Ri
IL10-LR
STAT1
STAT1p
Phosi
Phos
STAT3
STAT3p
STAT1p
STAT1p
STAT1p_Dm
STAT1p
STAT1
STAT3p
STAT3p
STAT3p_Dm
STAT3p
STAT3
SOCS3
SOCS1
B
Model
Data
[STAT3 p] / [STAT3 B]
time[min]
C
[STAT1 p] / [STAT1 B]
time[min]
D
[SOCS1 I] / [SOCS1 B]
time[min]

Figure 3

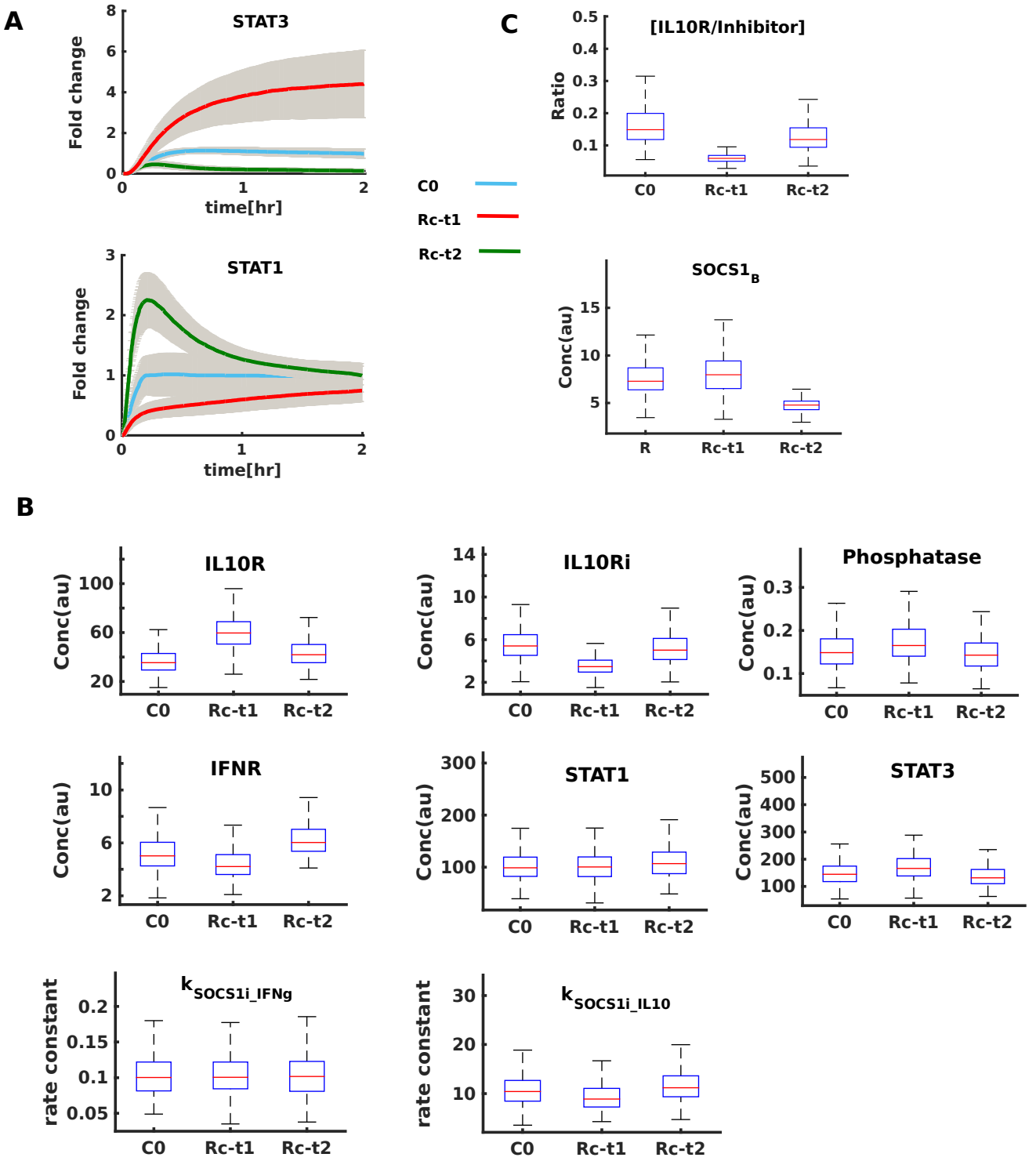
A
STAT3
Fold change
time[hr]
STAT1
Fold change
time[hr]
C0
Rc-t1
Rc-t2
C
[IL10R/Inhibitor]
Ratio
C0
Rc-t1
Rc-t2
SOCS1B
Conc(au)
R
Rc-t1
Rc-t2
B
IL10R
IL10Ri
Phosphatase
IFNR
STAT1
STAT3
Conc(au)
kSOCS1i_IFNg
kSOCS1i_IL10
rate constant
C0
Rc-t1
Rc-t2

Figure 4

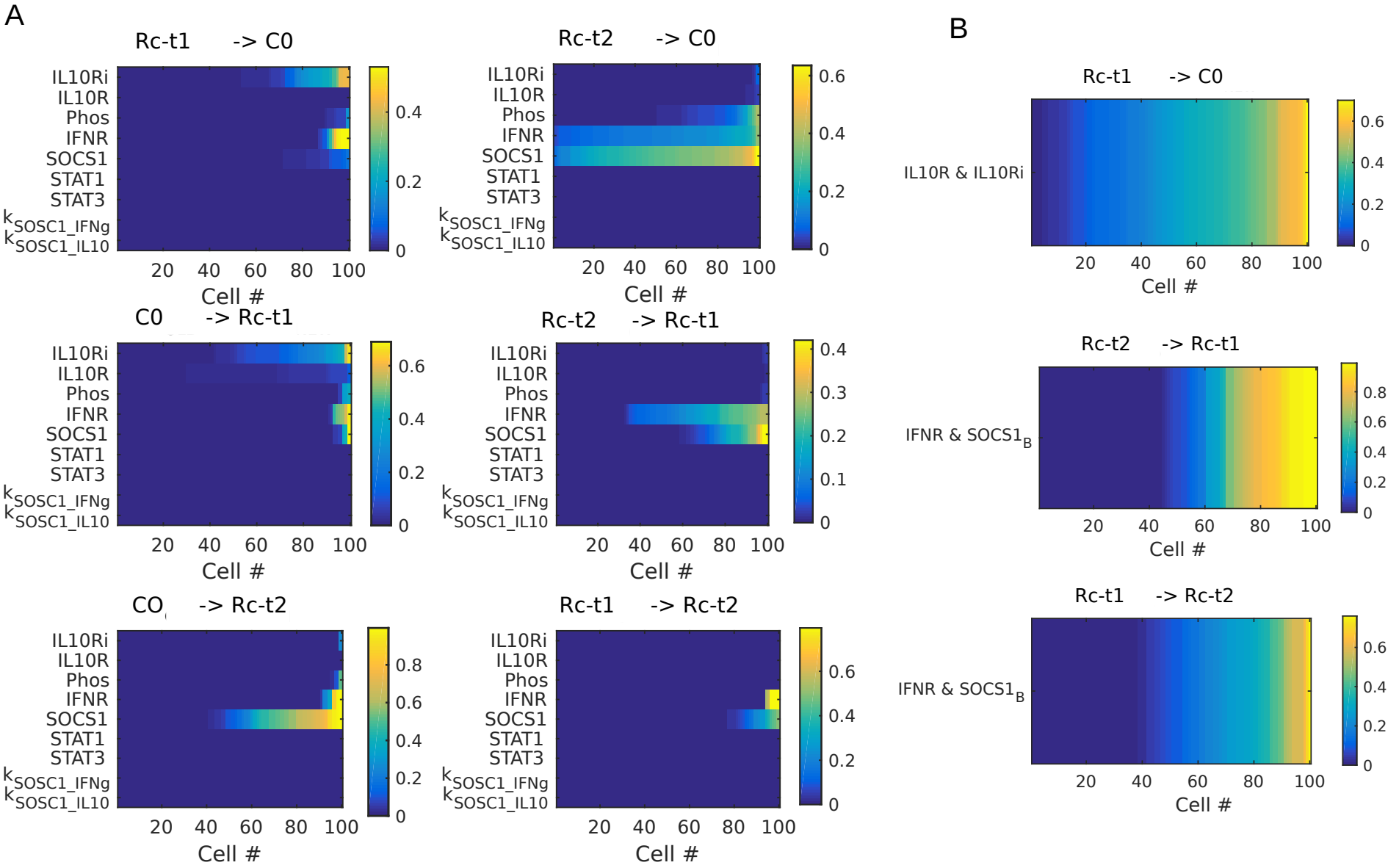
A
Rc-t1 -> C0
Rc-t2 -> C0
C0 -> Rc-t1
Rc-t2 -> Rc-t1
CO -> Rc-t2
Rc-t1 -> Rc-t2
IL10Ri
IL10R
Phos
IFNR
SOCS1
STAT1
STAT3
kSOSC1_IFNg
kSOSC1_IL10
Cell #
B
Rc-t1 -> C0
IL10R & IL10Ri
Rc-t2 -> Rc-t1
IFNR & SOCS1B
Rc-t1 -> Rc-t2
IFNR & SOCS1B
Cell #

Figure 5